THE JOURNAL OF PHYSICAL CHEMISTRY A LETTERS

2006, *110,* 2579−2582
Published on Web 02/03/2006

Spatial Quantification of Mn^{2+} and Mn^{3+} Concentrations in the Mn-Catalyzed 1,4-Cyclohexanedione/Acid/Bromate Reaction Using Magnetic Resonance Imaging

Melanie M. Britton[†]

Magnetic Resonance Research Centre, Department of Chemical Engineering, University of Cambridge, New Museums Site, Pembroke Street, Cambridge CB2 3RA, U.K.

Received: December 9, 2005; In Final Form: January 20, 2006

This paper presents a magnetic resonance imaging (MRI) method for quantifying the spatial concentrations of the paramagnetic species Mn^{2+} and Mn^{3+}, during pattern formation, in the manganese-catalyzed 1,4-cyclohexanedione−acid−bromate reaction. The relaxivity of each species was measured, which enabled their concentration to be calculated from nuclear magnetic resonance T_2 relaxation times. Images were acquired using the fast spin−echo imaging method RARE. By determining the relation, in these experiments, between signal intensity and T_2 relaxation time, it was possible to produce T_2 maps from the images. These T_2 maps were then used to produce concentration maps for the oxidized (Mn^{3+}) and reduced (Mn^{2+}) states of the catalyst.

Introduction

Chemical waves or fronts form in reactions where there is a coupling between autocatalysis and diffusion. The most studied pattern forming reaction is the Belousov−Zhabotinsky (BZ) reaction,[1] which can produce a wide variety of spatio-temporal behavior including trigger, target and spiral waves. Many studies of this system have measured the velocity as a function of reactant concentration. However, to fully test *reaction−diffusion* models, it is important to be able to spatially quantify the concentration of species. Direct spatial measurements have been made of ferroin[2] and cerium[3] concentrations in BZ systems using spectrophotometric experiments. Wood and Ross[2] probed 1-dimensional trigger waves by measuring the concentration of ferroin in the BZ reaction using a linear photodiode array. Nagy-Ungvarai and co-workers[3] used a UV-sensitive 2D spectrophotometer to measure concentration profiles in the cerium-catalyzed BZ reaction, and Vidal and Pagola[4] used digital video techniques to probe 2D waves in the ferroin-catalyzed BZ reaction.

These optical methods are limited, however, to visualization of catalyst concentrations in 2D layers and in transparent media. This paper reports the use of an alternative technique for the measurement of catalyst concentrations: magnetic resonance imaging (MRI). The advantage with this technique is that it is able to probe 3D volumes, optically opaque systems and indicators with no detectable color change. Similar MRI techniques have been used in medical research to quantify transition metal ion or gadolinium contrast agent concentrations in biological systems.[5,6] Previously, Cross and co-workers[7] have also used MRI to measure manganese concentrations in a BZ reaction. They used a 64-echo CPMG imaging sequence, where one image was acquired for each echo. Using this method, accurate T_2 maps are produced, which can be used to quantify catalyst concentration. However, experiments can take on the order of minutes to acquire and for many chemical wave systems this is too slow, as waves can move several millimeters during data acquisition. Therefore a faster method is required.

This paper presents the first application of a fast spin−echo imaging experiment (RARE[8]) to measure paramagnetic ion concentrations during chemical pattern formation. This technique has been used successfully to evaluate moisture content in rice grains during cooking,[9] using T_2 relaxation times, determined from the signal intensities of pixels in the image. Using this imaging method Mn^{2+} and Mn^{3+} concentration maps were produced for patterns formed in the manganese-catalyzed 1,4-cyclohexanedione−acid−bromate reaction (CHD).[10] MRI is the only technique able to probe concentration profiles of manganese in this reaction, as the complex does not exhibit strong color changes. Two-dimensional (2D) concentration maps were created, from 3D volumes, in less than 1 s.

Experimental Section

CHD Reaction. The reacting solution was 2.5 M H_2SO_4 (Aldrich), 0.1 M 1,4-cyclohexanedione (Aldrich), 0.1 M $NaBrO_3$ (Fluka) and 2.75×10^{-4} manganese(III) acetate (Aldrich). All reactants were used with no further purification. Manganese sulfate, which has been used previously in this system,[11] was not used as it was not easy to produce an oxidized solution, preventing the measurement of the NMR *relaxivity* of the Mn^{3+} solution. Indeed, addition of bromate does not give full conversion because reaction step R1 is highly reversible, so full

$$Mn^{2+} + BrO_2^{\bullet} + H^+ \Leftrightarrow Mn^{3+} + HBrO_2 \qquad (R1)$$

conversion is not possible and the degree of conversion was dependent on the starting concentration of $MnSO_4$. Oxidation

[†] Present address: School of Chemistry, University of Birmingham, Edgbaston, Birmingham, B15 2TT, U.K. E-mail: m.m.britton@bham.ac.uk.

10.1021/jp057201f CCC: $33.50

with PbO_2, which has been successfully used with ferroin,[12] produced erratic conversion.

Nuclear Magnetic Resonance Techniques. For an introduction to the principles of magnetic resonance, the reader is referred elsewhere.[13] The NMR spectrometer used was a Bruker Biospin DMX-300, which comprised a 7.0 T superconducting magnet, operating at a proton resonance frequency of 300 MHz, equipped with shielded and water-cooled gradient coils. All NMR experiments were done at a temperature of 21 ± 0.2 °C, using a 25 mm radio frequency coil. NMR data were analyzed using the software package PROSPA.[14]

NMR Relaxation Time Experiments. Relaxation experiments were performed to measure the transverse, T_2, relaxation times of solutions containing oxidized (Mn^{3+}) and reduced (Mn^{2+}) states of the transition metal ion complex. A solution of Mn^{3+} ions was produced by dissolving manganese(III) acetate in 2.5 M sulfuric acid and the reduced solution was produced by adding 0.1 M 1,4-cyclohexanedione (CHD). Manganese(III) is known to be unstable,[15] disproportionating to Mn(II) and Mn(IV); however, these experiments were performed in strong sulfuric acid conditions and complexing anions such as SO_4^{2-} are known to stabilize Mn(III) in aqueous solutions.[16] Degradation of Mn(III) was not observed during experiments, though fresh solutions were made prior to every experiment.

Carr−Purcell−Meiboom−Gill (CPMG) experiments[13] were used to measure the T_2 for the two solutions at different concentrations. Typically, 128 echoes were collected for each experiment, with an echo spacing of 1−4 ms, ensuring that data were collected for a minimum of ($5T_2$) s.

Imaging Experiments. Images were obtained using the fast spin−echo imaging sequence RARE, details of which can be found elsewhere.[8,17] This sequence is based on a single excitation, multi-echo acquisition and image contrast is produced through differences in spin density and T_2 relaxation time differences. Images were orientated vertically and were made up of 128 × 32 pixel arrays, corresponding to the vertical and horizontal dimensions, with respective fields-of-view of 50.0 mm × 6.2 mm. Images had a slice thickness of 1 mm and were positioned in the center of the tube. A RARE factor (the number of echoes acquired per excitation) of 32 was used, producing an effective echo time of 52.1 ms. The repetition time between successive excitations was 2.5 s, which allowed the magnetization of the system to fully relax before the next excitation pulse. Each image was acquired from a single excitation and only one signal acquisition was required. An image, therefore, took approximately 100 ms to acquire. Water molecules surrounding Mn^{3+} ions have a longer relaxation time than those surrounding Mn^{2+} ions, resulting in greater (brighter) signal intensity in regions where Mn^{3+} ions predominate.

Results and Discussion

Plots of relaxation rate ($1/T_2$) against concentration gave straight lines for both the oxidized (Mn^{3+}) and reduced (Mn^{2+}) manganese acetate solutions. Fits to each line[18] are given in

$$\frac{1}{T_{2_{\mathrm{Mn(II)}}}} = 126.7 \times 10^3[\mathrm{Mn}^{2+}] + 0.44 \qquad (1a)$$

$$\frac{1}{T_{2_{\mathrm{Mn(III)}}}} = 16.3 \times 10^3[\mathrm{Mn}^{3+}] + 1.62 \qquad (1b)$$

where $[Mn^{2+}]$ and $[Mn^{3+}]$ are the concentrations of the oxidized and reduced solutions, respectively, in M, and $1/T_{2_{\mathrm{Mn(II)}}}$; $1/T_{2_{\mathrm{Mn(III)}}}$ are the corresponding solvent molecule relaxation rates, in s^{-1}.

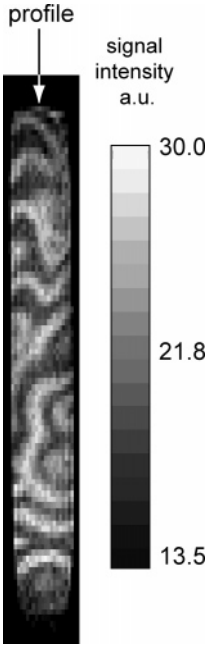

Figure 1. MRI RARE image of pattern formation in the manganese-catalyzed CHD reaction. The image is acquired using a 128 × 32 pixel array, with a RARE factor of 32, slice thickness of 1 mm and a receiver gain of 64. The area of the image displayed is 36.5 mm (vertically) by 5 mm (horizontally). The image is taken 6 min after the start of pattern formation.

The constant in each fit is the diamagnetic contribution to the relaxation rate from the solvent molecules. The linear dependence of relaxation rate with concentration is given by the *relaxivity* of the paramagnetic species.[19] As both metal ion complexes are paramagnetic, they reduce the relaxation time for water molecules surrounding them. However, as Mn^{2+} has one more unpaired electron that Mn^{3+}, its relaxivity is greater.

In a solution containing both Mn^{2+} and Mn^{3+} ions, as is found in the CHD reaction, the observed relaxation rate will be a sum of relaxation rates of the diamagnetic solvent molecules and the paramagnetic contribution from the Mn^{2+} and Mn^{3+} ions,[16] depending on their relative concentrations (eq 2).

$$\frac{1}{T_2} = \frac{1}{T_{2_{\mathrm{Mn(II)}}}} + \frac{1}{T_{2_{\mathrm{Mn(III)}}}} + \frac{1}{T_{2_{\mathrm{sol}}}} \qquad (2)$$

As the total concentration of manganese ions remains constant ($[Mn]_0 = [Mn^{2+}] + [Mn^{3+}]$), it is possible to combine eqs 1a,b and 2 to produce an expression giving the concentration of reduced or oxidized ions for an observed relaxation rate (eqs 3a,b).

$$\frac{1}{T_{2_{\mathrm{obs}}}} = 16.3 \times 10^3[\mathrm{Mn}]_0 + 110.4 \times 10^3[\mathrm{Mn}^{2+}] + 1.02 \qquad (3a)$$

$$\frac{1}{T_{2_{\mathrm{obs}}}} = 126.7 \times 10^3[\mathrm{Mn}]_0 - 110.4 \times 10^3[\mathrm{Mn}^{3+}] + 1.02 \qquad (3b)$$

In these equations an average for the diamagnetic contribution from the solvent molecules (eqs 1a,b) has been used. So, by measuring the T_2 of the system it is possible to measure concentrations of Mn^{2+} and Mn^{3+} ions.

Figure 1 shows a typical RARE image obtained during pattern formation in the CHD reaction. As this experiment collects a

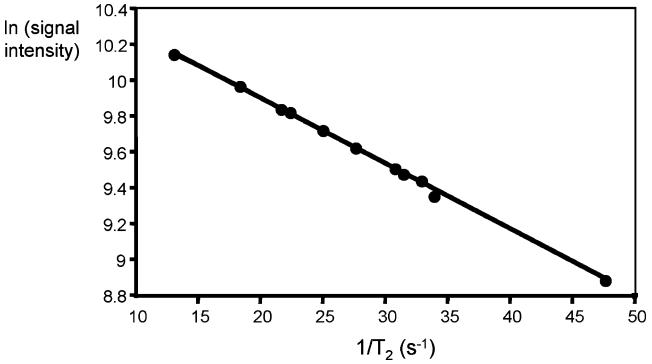

Figure 2. Plot of the natural logarithm of signal intensity (SI) against relaxation rate, $1/T_2$, from a series of RARE images of solutions of different T_2, using the same imaging parameters as Figure 1.

series of echoes following an excitation pulse, the image is T_2-weighted. So, regions of high (bright) signal intensity are related to longer relaxation times (where Mn^{3+} ions predominate) than regions of low (dark) signal intensity (where Mn^{2+} ions predominate).

In the RARE experiment,[8,17] the effect of relaxation on the signal intensity in a pixel is complicated; however, a linear relationship between the natural logarithm of signal intensity (ln(SI)) and relaxation rate ($1/T_2$) can be approximated. This is illustrated in the plot shown in Figure 2, where ln(SI), from RARE images of a range of solutions of different T_2, is plotted against $1/T_2$. The data produce a straight line and a fit of this slope gives

$$\ln(\mathrm{SI}) = \frac{-0.036}{T_2} + 10.6 \qquad (4)$$

This approximation was only tested over a range of T_2 and T_1 times between 15−80 ms and 350−700 ms, respectively. However, it may also hold true in other systems and over a greater range of relaxation times, though this would need to be tested by acquiring calibration data over the full range of relaxation times exhibited by that system. Also, this relationship can only be applied to images that have been acquired using the same imaging parameters, e.g., RARE factor, receiver gain, echo time. Other experiments using different parameters would need to be calibrated for that setup, over the range of relaxation times exhibited in that system.

Using the signal intensities obtained from the image in Figure 1, it was possible to extract an average T_2 value for solvent molecules within each pixel. Following this, the T_2 relaxation times were then converted into Mn^{2+} and Mn^{3+} concentrations, using eqs 3a,b. Figure 3 gives the relaxation times and manganese concentrations for a line extracted from the image shown in Figure 1. T_2 and concentration maps were also generated from the RARE MRI image of patterns in a manganese-catalysed CHD reaction and have been displayed, in Figure 4. Here different color scales have been used for the relaxation time and concentration maps, to maximize image contrast for those parameters.

In the oscillations of Mn^{2+} and Mn^{3+}, it can be seen that there is not full conversion between the two oxidative states during the reaction. This has also been seen in the cerium-[3] and ferroin-catalyzed[2] BZ reactions. The degree of conversion is, however, greater on average than that seen in the cerium-catalyzed BZ system, but similar to the ferroin-catalyzed system. Although the degree of image contrast produced by a reaction can be estimated from the relative relaxivities of the reduced and oxidized solutions, the actual image contrast is dependent on this conversion. So, increased image contrast would require greater conversion.

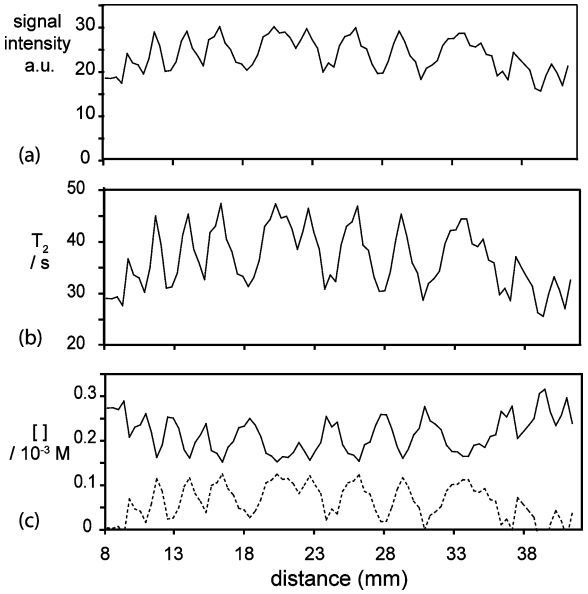

Figure 3. Plots of (a) signal intensity (SI), (b) T_2 relaxation time and (c) concentration ([ ]) for Mn^{2+} (—) and Mn^{3+} (---) against time, for the image profile shown in Figure 1. Errors in the calculated T_2 relaxation times and concentrations are $\pm 1 \times 10^{-3}$ s and $\pm 5 \times 10^{-6}$ M, respectively. These errors are slightly greater at the top ($z > 38$ mm) and bottom ($z < 10$ mm) of the image due to pulse imperfections and the decrease in field gradient homogeneity in these outer areas of the observable region.

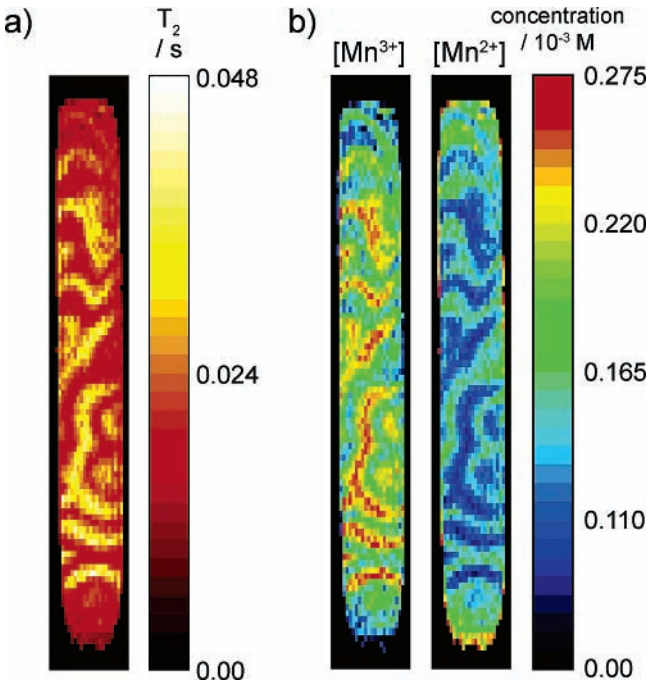

Figure 4. (a) T_2 and (b) Mn^{2+} and Mn^{3+} concentration maps for patterns in a manganese-catalyzed CHD reaction, produced from the image shown in Figure 1.

Conclusions

This paper presents a method for quantifying the local concentrations of paramagnetic manganese species, through determination of T_2 relaxation times. This method could also be applied to the quantification of local concentrations of other paramagnetic ions, such as iron, cobalt, cerium or copper, for

example. This technique has advantages over optical methods because 3D volumes and optically opaque systems can be probed, as well as transition metal ions with no visible color change. To produce concentration maps of the catalyst, the relationship between signal intensity and T_2 needs to be calibrated, for a set of imaging parameters, and the relaxivity of the paramagnetic species needs to be measured.

Extension of this work to gels and porous media is possible. However, care must be taken that variations in T_2 associated with the medium, and in particular inhomogeneous variations associated with the heterogeneity of the medium, are not misinterpreted as changes in transition metal ion concentration.

Acknowledgment. M.M.B. thanks EPSRC for an Advanced Research Fellowship, Prof. Lynn F. Gladden and her group at the MRRC, Cambridge University for support and Dr. Andrew Sederman and Dr. Mick Mantle for helpful discussions.

References and Notes

(1) Zaikin, A. N.; Zhabotinsky, A. M. *Nature* **1970**, *225*, 535.
(2) Wood, P. M.; Ross, J. *J. Chem. Phys.* **1985**, *82*, 1924.
(3) Nagy-Ungvarai, Z.; Muller, S. C.; Tyson, J. J.; Hess, B. *J. Phys. Chem.* **1989**, *93*, 2760.
(4) Pagola, A.; Vidal, C. *J. Phys. Chem.* **1987**, *91*, 501.
(5) Clark, P. R.; Chua-anusorn, W.; St Pierre, T. G. *Magn. Reson. Med.* **2003**, *49*, 572.
(6) Fritz-Hansen, T.; Rostrup, E.; Ring, P. B.; Larsson, H. B. W. *Magn. Reson. Imag.* **1998**, *16*, 893.
(7) Cross, A. The Development of Three-Dimensional Magnetic Resonance Imaging of the Belousov−Zhabotinsky Reaction. Ph.D. Thesis, The University of New Brunswick, 1998.
(8) Hennig, J.; Naureth, A.; Friedburg, H. *Magn. Reson. Med.* **1986**, *3*, 823.
(9) Mohoric, A.; Vergeldt, F.; Gerkema, E.; de Jager, A.; van Duynhoven, J.; van Dalen, G.; Van As, H. *J. Magn. Reson.* **2004**, *171*, 157.
(10) Kurin-Csörgei, K.; Szalai, I.; Körös, E. *Reac. Kinet. Catal. Lett.* **1995**, *54*, 217.
(11) Britton, M. M. *J. Phys. Chem. A* **2003**, *107*, 5033.
(12) Szalai, I.; Kurin-Csorgei, K.; Epstein, I. R.; Orban, M. *J. Phys. Chem. A* **2003**, *107*, 10074.
(13) Callaghan, P. T. *Principles of Nuclear Magnetic Resonance Microscopy*; Oxford University Press: Oxford, NY, 1991.
(14) Magtritek. Prospa; http://www.magritek.com/prospa.html.
(15) Meyer, J.; Marek, J. *Z. Anorg. Chem* **1924**, *133*, 325.
(16) Cotton, F. A.; Wilkinson, G. *Advanced Inorganic Chemistry*, 5th ed.; Wiley: New York.
(17) Hennig, J. *J. Magn. Reson.* **1988**, *78*, 397.
(18) Hansen, E. W.; Ruoff, P. *J. Phys. Chem.* **1989**, *93*, 264.
(19) Lauffer, R. B. *Chem. Rev.* **1987**, *87*, 901.